

Multiple Insertion of Unsaturated Molecules into the Zr–N Bonds of $[\eta^5\text{-}\sigma\text{-Me}_2\text{A}(\text{C}_9\text{H}_6)(\text{C}_2\text{B}_{10}\text{H}_{10})]\text{Zr}(\text{NMe}_2)_2$ (A = C, Si)

Haiping Wang, Hung-Wing Li, and Zuowei Xie*

Department of Chemistry, The Chinese University of Hong Kong, Shatin, New Territories, Hong Kong, China

Received June 3, 2003

The compounds $[\eta^5\text{-}\sigma\text{-Me}_2\text{A}(\text{C}_9\text{H}_6)(\text{C}_2\text{B}_{10}\text{H}_{10})]\text{Zr}(\text{NMe}_2)_2$ (A = C, Si) reacted with CS_2 , PhCN , $\text{CH}_2=\text{CHCN}$, $n\text{BuNCS}$, and PhNCO to give the mono-, di-, and triinsertion products, depending upon the substrates. These unsaturated substances inserted exclusively into the Zr–N bonds, and the Zr–C(cage) bond remains intact in all reactions. It is believed that the preference of Zr–N over Zr–C(cage) insertion is governed by steric factors. The metal amide compounds also initiated the polymerization of $\text{CH}_2=\text{CHCN}$ to produce poly(acrylonitrile) and catalyzed the trimerization of PhNCO . On the other hand, they reacted with methyl methacrylate to afford $[\{\eta^5\text{-}\sigma\text{-Me}_2\text{A}(\text{C}_9\text{H}_6)(\text{C}_2\text{B}_{10}\text{H}_{10})\}\text{Zr}(\text{OCH}_3)(\mu\text{-OCH}_3)]_2$ and $\text{CH}_2=\text{C}(\text{Me})\text{CONMe}_2$. All insertion products were fully characterized by various spectroscopic data, elemental analyses, and X-ray diffraction studies.

Introduction

Since the report of a new generation of group 4 metallocene precatalysts containing bridged cyclopentadienyl ligands, there has been increasing interest in the development of the chemistry of such *ansa*-metallocene systems.¹ Replacement of one cyclopentadienyl ring by an amido group reduces the overall valence electrons and the steric congestion at an electrophilic d^0 metal center, leading to so-called constrained-geometry ligands.² Researchers at Dow Chemical³ and Exxon⁴ have utilized these types of ligand systems to develop a new generation of constrained-geometry Ziegler–Natta olefin polymerization precatalysts, $[\text{R}'_2\text{Si}(\eta^5\text{-C}_5\text{R}_4)(\text{NR}'')]\text{MX}_2$ (M = Ti, Zr, Hf; R = alkyl; R', R'' = alkyl, aryl; X = alkyl, halide). It is believed that the $[\text{R}'_2\text{-Si}(\eta^5\text{-C}_5\text{R}_4)(\text{NR}'')]\text{M}$ fragment remains intact during the olefin polymerization: that is, the olefin inserts exclusively into the M–C bond. Such a reactivity pattern may be altered if the property of monomers is changed. For example, both the Zr–Me and Zr–N bonds in $[\text{Me}_2\text{Si}(\eta^5\text{-C}_5\text{Me}_4)(\text{NBu}^t)]\text{ZrMe}_2$ can react with excess CO_2 , leading to the formation of carboxylation products.⁵ The

Ti–N bond in $[\text{Me}_2\text{Si}(\eta^5\text{-C}_5\text{H}_4)(\text{NBu}^t)]\text{TiCl}_2$ also shows reaction toward CO_2 .⁶ Although the insertion of small molecules such as CO_2 , isocyanides, isocyanates, and $\text{CH}_2=\text{CHCN}$ into the Zr–C,⁷ Zr–N,⁸ and Zr–Si⁹ bonds has been documented, studies on the relative activity of Zr–N/Zr–C bonds are very rare.^{5,10}

We have recently developed a new class of constrained-geometry ligands bearing a carboanion functionality, $[\text{Me}_2\text{A}(\text{C}_5\text{H}_4)(\text{C}_2\text{B}_{10}\text{H}_{10})]^{2-}$ (A = C,¹¹ Si¹²), $[\text{Me}_2\text{A}(\text{C}_9\text{H}_6)(\text{C}_2\text{B}_{10}\text{H}_{10})]^{2-}$ (A = C,¹³ Si¹⁴), and $[\text{Pr}_2\text{NB}(\text{C}_9\text{H}_6)(\text{C}_2\text{B}_{10}\text{H}_{10})]^{2-}$.¹⁵ Group 4 metal amide/chloride compounds with these ligand systems are active catalysts for ethylene polymerization upon activation with methylalumoxane.^{16,17} Do these compounds react with small molecules

* To whom correspondence should be addressed. Fax: (852)-26035057. Tel: (852)26096269. E-mail: xzie@cuhk.edu.hk.

(1) For reviews, see: (a) Britovsek, G. J. P.; Gibson, V. C.; Wass, D. F. *Angew. Chem., Int. Ed.* **1999**, *38*, 428. (b) Kaminsky, W.; Arndt, M. *Adv. Polym. Sci.* **1997**, *127*, 144. (c) Bochmann, M. *J. Chem. Soc., Dalton Trans.* **1996**, 255. (d) Kaminsky, W. *Macromol. Chem. Phys.* **1996**, *197*, 3907. (e) Brintzinger, H. H.; Fisher, D.; Mülhaupt, R.; Rieger, B.; Waymouth, R. M. *Angew. Chem., Int. Ed. Engl.* **1995**, *34*, 1143. (f) Möhring, R. C.; Coville, N. J. *J. Organomet. Chem.* **1994**, *479*, 1. (g) Marks, T. J. *Acc. Chem. Res.* **1992**, *25*, 57.

(2) For reviews, see: (a) Siemeling, U. *Chem. Rev.* **2000**, *100*, 1495. (b) Jutzi, P.; Siemeling, U. *J. Organomet. Chem.* **1995**, *500*, 175. (c) Okuda, J. *Comments Inorg. Chem.* **1994**, *16*, 185.

(3) Stevens, J. C.; Timmers, F. J.; Wilson, D. R.; Schmidt, G. F.; Nickias, P. N.; Rosen, R. K.; Knight, G. W.; Lai, S. Eur. Patent 416 815, 1990.

(4) (a) Canich, J. M. Eur. Patent 420 436, 1991. (b) Canich, J. M.; Hlatky, G. G.; Turner, H. W. U.S. Patent 542 236, 1990.

(5) Kloppenburg, L.; Petersen, J. L. *Organometallics* **1996**, *15*, 7.

(6) Ciruelos, S.; Cuenca, T.; Gómez, R.; Gómez-Sal, P.; Manzanero, A.; Royo, P. *Organometallics* **1996**, *15*, 5577.

(7) (a) Negishi, E.; Montchamp, J.-L. In *Metallocenes: Synthesis, Reactivity, Applications*; Togni, A., Halterman, R. L., Eds.; Wiley-VCH: New York, 1998; Vol. 1, p 241. (b) Durfee, L. D.; Rothwell, I. P. *Chem. Rev.* **1988**, *88*, 1059.

(8) (a) Lappert, M. F.; Power, P. P.; Sanger, A. R.; Srivastava, R. C. *Metal and Metalloid Amides*; Ellis Horwood: Chichester, U.K., 1980; Chapter 10. (b) Walsh, P. J.; Carney, M. J.; Bergman, R. G. *J. Am. Chem. Soc.* **1991**, *113*, 6343.

(9) (a) Wu, Z.; McAlexander, L. H.; Diminnie, J. B.; Xue, Z. *Organometallics* **1998**, *17*, 4853. (b) Wu, Z.; Diminnie, J. B.; Xue, Z. *Organometallics* **1999**, *18*, 1002.

(10) (a) Andersen, R. A. *Inorg. Chem.* **1979**, *18*, 2928. (b) Gately, D. A.; Norton, J. R.; Goodson, P. A. *J. Am. Chem. Soc.* **1995**, *117*, 986.

(11) (a) Xie, Z.; Chui, K.; Yang, Q.; Mak, T. C. W. *Organometallics* **1999**, *18*, 3947. (b) Chui, K.; Yang, Q.; Mak, T. C. W.; Xie, Z. *Organometallics* **2000**, *19*, 1391.

(12) (a) Xie, Z.; Wang, S.; Zhou, Z.-Y.; Xue, F.; Mak, T. C. W. *Organometallics* **1998**, *17*, 489. (b) Xie, Z.; Wang, S.; Zhou, Z.-Y.; Mak, T. C. W. *Organometallics* **1998**, *17*, 1907. (c) Xie, Z.; Wang, S.; Zhou, Z.-Y.; Mak, T. C. W. *Organometallics* **1999**, *18*, 1641.

(13) Wang, S.; Yang, Q.; Mak, T. C. W.; Xie, Z. *Organometallics* **2000**, *19*, 334.

(14) (a) Xie, Z.; Wang, S.; Yang, Q.; Mak, T. C. W. *Organometallics* **1999**, *18*, 2420. (b) Wang, S.; Yang, Q.; Mak, T. C. W.; Xie, Z. *Organometallics* **1999**, *18*, 4478. (c) Wang, S.; Yang, Q.; Mak, T. C. W.; Xie, Z. *Organometallics* **1999**, *18*, 1578.

(15) Zi, G.; Li, H.-W.; Xie, Z. *Organometallics* **2002**, *21*, 1136.

(16) Wang, H.; Wang, Y.; Li, H.-W.; Xie, Z. *Organometallics* **2001**, *20*, 5110.

bearing an activated C=C double bond or other multiple bonds? Reactivity patterns of compounds involving both group 4 metal M–N and M–C(cage) bonds, to our knowledge, have not been investigated yet. The complexes $[\eta^5\text{-}\sigma\text{-Me}_2\text{A}(\text{C}_9\text{H}_6)(\text{C}_2\text{B}_{10}\text{H}_{10})]\text{Zr}(\text{NMe}_2)_2$ (A = C (**1a**), Si (**1b**)) offer a unique opportunity to observe the direct competition between amido and carboranyl ligands in the migration step and to study whether amido or carboranyl ligand migration is preferred. We report in this paper our investigation on the reactions of **1a,b** with CS₂, PhCN, CH₂=CHCN, ⁿBuNCS, PhNCO and methyl methacrylate (MMA).

Experimental Section

General Procedures. All experiments were performed under an atmosphere of dry nitrogen with the rigid exclusion of air and moisture using standard Schlenk or cannula techniques or in a glovebox. All organic solvents were freshly distilled from sodium benzophenone ketyl immediately prior to use. Compounds **1a,b** were prepared according to the literature methods.¹⁶ All other chemicals were purchased from Aldrich Chemical Co. and were freshly distilled prior to use. Infrared spectra were obtained from KBr pellets prepared in the glovebox on a Nicolet Magna 550 Fourier transform spectrometer. ¹H and ¹³C NMR spectra were recorded on a Bruker DPX 300 spectrometer at 300.13 and 75.47 MHz, respectively. ¹¹B NMR spectra were recorded on a Varian Inova 400 spectrometer at 128.32 MHz. All chemical shifts are reported in δ units with reference to internal or external TMS (0.00 ppm) or with respect to the residual protons of the deuterated solvents for proton and carbon chemical shifts and to external BF₃·OEt₂ (0.00 ppm) for boron chemical shifts. Elemental analyses were performed by MEDAC Ltd, Brunel University, Middlesex, U.K.

Preparation of $[\eta^5\text{-}\sigma\text{-Me}_2\text{C}(\text{C}_9\text{H}_6)(\text{C}_2\text{B}_{10}\text{H}_{10})]\text{Zr}[\text{N}=\text{C}(\text{Ph})\text{NMe}_2]_2$ (2a**).** To a toluene (20 mL) solution of $[\eta^5\text{-}\sigma\text{-Me}_2\text{C}(\text{C}_9\text{H}_6)(\text{C}_2\text{B}_{10}\text{H}_{10})]\text{Zr}(\text{NMe}_2)_2$ (**1a**; 240 mg, 0.5 mmol) was added dropwise a toluene (10 mL) solution of PhCN (110 mg, 1.0 mmol) at –30 °C with stirring. The mixture was warmed to room temperature and stirred for 5 h. After filtration, the resulting clear orange solution was concentrated under vacuum to about 8 mL. **2a** was isolated as yellow crystals after this solution stood at –30 °C for 3 days (280 mg, 82%). ¹H NMR (pyridine-*d*₅): δ 8.09 (d, *J* = 8.1 Hz, 1H), 6.98 (dd, *J* = 7.8 and 8.1 Hz, 1H), 6.89 (dd, *J* = 8.1 and 7.8 Hz, 1H), 6.77 (d, *J* = 3.3 Hz, 1H), 6.65 (d, *J* = 8.1 Hz, 1H), 5.87 (d, *J* = 3.3 Hz, 1H) (C₉H₆), 7.41 (s, 2H), 7.33 (d, *J* = 6.9 Hz, 4H), 7.19 (m, 4H) (C₆H₅), 2.78 (s, 6H), 2.60 (s, 6H) (N(CH₃)₂), 1.96 (s, 3H), 1.74 (s, 3H) ((CH₃)₂C). ¹³C NMR (pyridine-*d*₅): δ 157.51, 156.12 (C=N), 139.59, 131.98, 127.62, 127.52, 127.32, 127.10, 126.82, 126.75, 124.84, 124.44, 123.58, 123.30, 122.17, 121.80, 118.32, 117.30, 107.23 (C₉H₆ + C₆H₅), 103.62, 96.65 (C₂B₁₀H₁₀), 37.84, 34.92, 33.05 (N(CH₃)₂), 44.14, 31.02, 22.15 ((CH₃)₂C). ¹¹B NMR (pyridine-*d*₅): δ –6.5 (4), –10.5 (6). IR (KBr, cm^{–1}): ν 3052 (w), 3016 (w), 2989 (w), 2920 (m), 2597 (vs), 2551 (vs), 1594 (vs), 1539 (vs), 1480 (s), 1439 (s), 1376 (vs), 1262 (m), 1209 (m), 1182 (w), 1132 (w), 1084 (m), 1024 (m), 994 (w), 913 (m), 813 (s), 778 (m), 740 (m), 702 (m), 665 (m), 558 (m). Anal. Calcd for C₃₂H₄₄B₁₀N₄Zr: C, 56.18; H, 6.48; N, 8.19. Found: C, 55.94; H, 6.59; N, 8.31.

Preparation of $[\eta^5\text{-}\sigma\text{-Me}_2\text{C}(\text{C}_9\text{H}_6)(\text{C}_2\text{B}_{10}\text{H}_{10})]\text{Zr}[\text{N}=\text{C}(\text{C}_2\text{H}_3)\text{NMe}_2]_2\cdot 2\text{C}_6\text{H}_5\text{CH}_3$ (3a**·(toluene)).** This compound was prepared as yellow crystals from **1a** (240 mg, 0.5 mmol) and acrylonitrile (53 mg, 1.0 mmol) in toluene using a procedure identical with that reported for **2a**. Yield: 130 mg (39%). ¹H NMR (pyridine-*d*₅): δ 8.15 (d, *J* = 8.4 Hz, 1H), 7.26 (m, 3H), 7.16 (m, 5H), 7.00 (d, *J* = 3.2 Hz, 1H), 6.90 (d, *J* = 3.2 Hz, 1H)

(C₉H₆ + C₆H₅CH₃), 6.11 (d, *J* = 4.4 Hz, 2H), 5.83 (m, 2H), 5.36 (m, 2H) (vinyl), 2.90 (s, 6H), 2.66 (s, 6H) (N(CH₃)₂), 2.20 (s, 3H) (C₆H₅CH₃), 2.02 (s, 3H), 1.85 (s, 3H) ((CH₃)₂C). ¹³C NMR (pyridine-*d*₅): δ 157.82, 156.43 (C=N), 139.64, 132.01, 127.84, 127.42, 127.22, 126.82, 124.93, 124.66, 123.36, 118.56, 107.99 (C₉H₆ + C₆H₅ + vinyl), 95.32 (C₂B₁₀H₁₀), 37.90, 35.23 (N(CH₃)₂), 44.32, 31.23, 22.10 ((CH₃)₂C). ¹¹B NMR (pyridine-*d*₅): δ –5.5 (4), –8.8 (6). IR (KBr, cm^{–1}): ν 3039 (w), 2952 (s), 2866 (m), 2778 (w), 2589 (vs), 2559 (vs), 2172 (m), 1635 (w), 1544 (vs), 1456 (s), 1259 (w), 1182 (m), 1149 (m), 1092 (m), 1047 (m), 798 (m), 741 (m), 698 (m), 622 (w), 537 (m), 514 (m). Anal. Calcd for C₃₁H₄₈B₁₀N₄Zr: C, 55.07; H, 7.16; N, 8.29. Found: C, 54.73; H, 7.28; N, 8.37.

Reaction of **3a with Excess CH₂=CHCN.** To a toluene solution (30 mL) of **3a**·(toluene) (20 mg, 0.03 mmol) was added CH₂=CHCN (320 mg, 6.0 mmol) at room temperature, and the reaction mixture was stirred for 1 h, giving a large amount of precipitate. The polymerization was terminated by addition of acidic ethanol. The white precipitate was filtered off and washed with ethanol and acetone. The resulting powder was finally dried in a vacuum oven at 80 °C overnight (230 mg, 72%). ¹H NMR (DMSO-*d*₆): δ 5.95 (br) (vinyl), 3.10 (br) (CH₂CHCN), 2.85 (s) (NMe₂), 2.05 (br) (CH₂CHCN). *M_n*(NMR) $\approx 1.5 \times 10^5$.

Preparation of $[\{\eta^5\text{-}\sigma\text{-Me}_2\text{C}(\text{C}_9\text{H}_6)(\text{C}_2\text{B}_{10}\text{H}_{10})\}\text{Zr}(\text{OCH}_3)(\mu\text{-OCH}_3)]_2\cdot 2\text{C}_6\text{H}_5\text{CH}_3$ (4a**·2(toluene)).** To a toluene (20 mL) solution of **1a** (240 mg, 0.5 mmol) was added dropwise a toluene (10 mL) solution of methyl methacrylate (100 mg, 1.0 mmol) with stirring at room temperature, and the mixture was stirred overnight. After removal of the precipitate, the clear yellow solution was concentrated under vacuum to about 10 mL, to which was added a few drops of *n*-hexane. **4a**·2C₆H₅CH₃ was isolated as colorless crystals after this solution stood at room temperature for 2 days (220 mg, 81%). ¹H NMR (pyridine-*d*₅): δ 8.24 (d, *J* = 8.4 Hz, 1H), 7.25 (m, 5H), 7.16 (m, 7H), 6.86 (d, *J* = 3.3 Hz, 1H), 6.73 (d, *J* = 8.4 Hz, 1H), 5.78 (d, *J* = 3.3 Hz, 1H) (C₉H₆ + C₆H₅CH₃), 4.22 (s, 3H), 3.44 (s, 3H) (OCH₃), 2.20 (s, 6H) (C₆H₅CH₃), 2.06 (s, 3H), 1.88 (s, 3H) ((CH₃)₂C). ¹³C NMR (pyridine-*d*₅): δ 143.15, 131.31, 127.30, 126.41, 124.23, 123.31, 123.12, 121.51, 120.23, 106.32 (C₉H₆ + C₆H₅CH₃), 96.34 (C₂B₁₀H₁₀), 60.12, 59.45 (OCH₃), 45.15, 31.67, 22.80 ((CH₃)₂C). ¹¹B NMR (pyridine-*d*₅): δ –4.2 (2), –6.1 (2), –9.6 (6). IR (KBr, cm^{–1}): ν 3098 (w), 2986 (m), 2946 (s), 2921 (s), 2824 (m), 2589 (vs), 2558 (vs), 1603 (w), 1458 (s), 1383 (m), 1336 (w), 1191 (m), 1139 (vs), 1092 (m), 1052 (m), 997 (s), 846 (w), 806 (s), 741 (s), 697 (m), 524 (m). Anal. Calcd for C₃₉H₆₄B₂₀O₄Zr₂ (**4a** + toluene): C, 47.05; H, 6.48. Found: C, 47.21; H, 6.69.

Preparation of $[\{\eta^5\text{-}\sigma\text{-Me}_2\text{Si}(\text{C}_9\text{H}_6)(\text{C}_2\text{B}_{10}\text{H}_{10})\}\text{Zr}(\text{OCH}_3)(\mu\text{-OCH}_3)]_2\cdot 2\text{THF}$ (4b**·2THF).** This compound was prepared as colorless crystals from **1b** (247 mg, 0.5 mmol) and methyl methacrylate (100 mg, 1.0 mmol) in toluene/THF using a procedure identical with that reported for **4a**: yield 201 mg (75%). ¹H NMR (pyridine-*d*₅): δ 8.09 (d, *J* = 8.1 Hz, 1H), 7.29 (m, 1H), 7.14 (m, 1H), 6.97 (d, *J* = 3.3 Hz, 1H), 6.92 (d, *J* = 8.1 Hz, 1H), 5.98 (d, *J* = 3.3 Hz, 1H) (C₉H₆), 4.26 (s, 3H) (OCH₃), 3.63 (m, 4H) (THF), 3.42 (s, 3H) (OCH₃), 1.59 (m, 4H) (THF), 0.85 (s, 3H), 0.69 (s, 3H) ((CH₃)₂Si). ¹³C NMR (pyridine-*d*₅): δ 137.35, 130.08, 128.73, 127.98, 125.08, 123.85, 121.18, 105.63, 104.45 (C₉H₆), 101.03, 83.86 (C₂B₁₀H₁₀), 65.11 (THF), 57.02, 55.55 (OCH₃), 29.32 (THF), –0.99, –1.29 ((CH₃)₂Si). ¹¹B NMR (pyridine-*d*₅): δ –1.8 (2), –4.0 (2), –7.2 (2), –9.4 (1), –11.05 (2), –13.46 (1). IR (KBr, cm^{–1}): ν 3020 (w), 2951 (m), 2915 (m), 2831 (m), 2571 (vs), 1602 (w), 1491 (w), 1446 (m), 1415 (w), 1258 (s), 1136 (vs), 1088 (s), 1048 (w), 995 (s), 892 (m), 806 (s), 732 (m), 685 (m), 521 (m). Anal. Calcd for C₃₄H₆₄B₂₀O₅Si₂Zr₂ (**4b** + THF): C, 40.52; H, 6.40. Found: C, 40.21; H, 6.69.

Preparation of $[\eta^5\text{-}\sigma\text{-Me}_2\text{C}(\text{C}_9\text{H}_6)(\text{C}_2\text{B}_{10}\text{H}_{10})]\text{Zr}(\eta^2\text{-S}_2\text{C-NMe}_2)_2\cdot 2\text{C}_6\text{H}_5\text{CH}_3$ (5a**·2(toluene)).** To a toluene (20 mL) solution of **1a** (240 mg, 0.5 mmol) was added dropwise a

toluene (10 mL) solution of CS₂ (90 mg, 1.2 mmol) at -30 °C with stirring. The mixture was warmed to room temperature and stirred overnight. After removal of the precipitate, the clear yellow solution was concentrated under vacuum to about 10 mL, to which was added a few drops of *n*-hexane. **5a**·2(toluene) was isolated as bright yellow crystals after this solution stood at room temperature for 5 days (360 mg, 88%). ¹H NMR (pyridine-*d*₅): δ 8.14 (d, *J* = 8.7 Hz, 1H), 7.63 (d, *J* = 8.4 Hz, 1H), 7.49 (dd, *J* = 6.9 and 8.7 Hz, 1H), 7.28 (m, 6H), 7.16 (m, 5H), 7.11 (d, *J* = 3.3 Hz, 1H), 6.72 (d, *J* = 3.3 Hz, 1H) (C₉H₆ + C₆H₅CH₃), 3.16 (s, 6H), 2.95 (s, 6H) (N(CH₃)₂), 2.20 (s, 6H) (C₆H₅CH₃), 1.91 (s, 3H), 1.77 (s, 3H) ((CH₃)₂C). ¹³C NMR (pyridine-*d*₅): δ 201.61, 199.15 (NCS₂), 137.35, 136.81, 135.80, 128.72, 127.98, 127.22, 126.21, 125.82, 125.07, 123.80, 122.12, 111.05 (C₉H₆ + C₆H₅CH₃), 106.00, 104.49 (C₂B₁₀H₁₀), 39.69, 39.38, 34.66, 32.60 (N(CH₃)₂), 43.92, 31.02, 20.63 ((CH₃)₂C), 22.00 (C₆H₅CH₃). ¹¹B NMR (pyridine-*d*₅): δ -4.9 (3), -7.6 (2), -10.1 (5). IR (KBr, cm⁻¹): ν 3032 (w), 2928 (m), 2862 (m), 2593 (vs), 2550 (vs), 1637 (w), 1519 (vs), 1457 (m), 1387 (vs), 1250 (m), 1207 (w), 1144 (s), 1048 (m), 987 (m), 813 (m), 737 (s), 696 (m), 574 (w). Anal. Calcd for C₂₇H₄₂B₁₀N₂S₄Zr (**5a** + toluene): C, 44.90; H, 5.86; N, 3.88. Found: C, 44.71; H, 5.77; N, 4.02.

Preparation of [η⁵:σ-Me₂Si(C₉H₆)(C₂B₁₀H₁₀)]Zr(η²-S₂-CNMe₂)₂ (5b**).** This compound was prepared as bright yellow crystals from **1b** (247 mg, 0.5 mmol) and CS₂ (90 mg, 1.2 mmol) in toluene using a procedure identical with that reported for **5a**: yield 261 mg (81%). ¹H NMR (pyridine-*d*₅): δ 7.97 (d, *J* = 8.4 Hz, 1H), 7.72 (d, *J* = 8.4 Hz, 1H), 7.40 (dd, *J* = 8.4 and 7.2 Hz, 1H), 7.26 (dd, *J* = 8.4 and 7.2 Hz, 1H), 7.13 (d, *J* = 3.3 Hz, 1H), 7.09 (d, *J* = 3.3 Hz, 1H) (C₉H₆), 3.16 (s, 6H), 2.93 (s, 6H) (N(CH₃)₂), 0.74 (s, 3H), 0.61 (s, 3H) ((CH₃)₂Si). ¹³C NMR (pyridine-*d*₅): δ 202.68, 200.34 (NCS₂), 139.18, 130.55, 129.81, 128.98, 128.84, 128.33, 127.85, 126.91, 109.92 (C₉H₆), 84.96 (C₂B₁₀H₁₀), 41.45, 41.13, 32.85, 23.99 (N(CH₃)₂), 0.24, 0.00 ((CH₃)₂Si). ¹¹B NMR (pyridine-*d*₅): δ 0.3 (2), -4.1 (4), -9.5 (4). IR (KBr, cm⁻¹): ν 3020 (w), 2955 (m), 2923 (m), 2858 (w), 2570 (vs), 1517 (vs), 1450 (m), 1388 (vs), 1254 (s), 1146 (s), 1091 (s), 1046 (m), 990 (m), 892 (s), 831 (s), 803 (m), 739 (m), 685 (m), 576 (w), 551 (w). Anal. Calcd for C₁₉H₃₄B₁₀N₂S₄SiZr: C, 35.31; H, 5.30; N, 4.34. Found: C, 35.43; H, 5.36; N, 4.57.

Preparation of [η⁵:σ-Me₂C(C₉H₆)(C₂B₁₀H₁₀)]Zr(η²-OC-(NMe₂)NPh)₂ (6a**).** To a toluene (20 mL) solution of **1a** (240 mg, 0.5 mmol) was added dropwise a toluene (10 mL) solution of PhNCO (120 mg, 1.0 mmol) at 0 °C with stirring. The mixture was warmed to room temperature and stirred overnight. Removal of the solvent gave a yellow solid. Recrystallization from CH₂Cl₂ at room temperature afforded **6a** as pale yellow crystals (318 mg, 89%). ¹H NMR (pyridine-*d*₅): δ 8.05 (d, *J* = 8.4 Hz, 1H), 7.69 (d, *J* = 8.4 Hz, 1H), 7.43 (m, 2H), 7.34 (m, 2H), 7.25 (m, 2H), 7.15 (m, 2H), 7.10 (m, 2H), 7.00 (m, 2H), 6.47 (d, *J* = 3.3 Hz, 1H), 6.32 (d, *J* = 3.3 Hz, 1H) (C₉H₆ + C₆H₅), 2.36 (s, 6H), 2.20 (s, 6H) (N(CH₃)₂), 1.88 (s, 3H), 1.62 (s, 3H) ((CH₃)₂C). ¹³C NMR (pyridine-*d*₅): δ 166.00, 163.60 (NCO), 146.29, 137.35, 136.42, 128.96, 128.72, 128.08, 127.98, 126.85, 126.16, 125.51, 125.15, 124.36, 124.17, 123.31, 122.95, 121.84, 117.85 (C₉H₆ + C₆H₅), 102.23, 100.69 (C₂B₁₀H₁₀), 36.48, 36.34, 34.52, 32.64 (N(CH₃)₂), 44.19, 31.03, 20.63 ((CH₃)₂C). ¹¹B NMR (pyridine-*d*₅): δ -5.0 (3), -7.8 (2), -10.7 (5). IR (KBr, cm⁻¹): ν 3057 (w), 3024 (w), 2952 (m), 2930 (m), 2873 (w), 2589 (vs), 2558 (vs), 1634 (w), 1565 (vs), 1490 (vs), 1446 (vs), 1407 (vs), 1306 (w), 1240 (m), 1208 (m), 1027 (m), 932 (w), 796 (m), 750 (m), 700 (m), 646 (m), 511 (w). Anal. Calcd for C₃₂H₄₄B₁₀N₄O₂Zr: C, 53.67; H, 6.19; N, 7.83. Found: C, 53.88; H, 6.23; N, 7.93.

Preparation of [η⁵:σ-Me₂Si(C₉H₆)(C₂B₁₀H₁₀)]Zr(η²-OC-(NMe₂)NPh)₂ (6b**).** This compound was prepared as colorless crystals from **1b** (247 mg, 0.5 mmol) and PhNCO (120 mg, 1.0 mmol) in toluene using a procedure identical with that reported for **6a**: yield 300 mg (82%). ¹H NMR (pyridine-*d*₅): δ 7.88 (d, *J* = 8.7 Hz, 1H), 7.80 (d, *J* = 8.7 Hz, 1H), 7.43 (m,

3H), 7.35 (m, 3H), 7.23 (m, 2H), 7.13 (m, 2H), 7.01 (m, 2H), 6.77 (d, *J* = 3.0 Hz, 1H), 6.43 (d, *J* = 3.0 Hz, 1H) (C₉H₆ + C₆H₅), 2.36 (s, 12H) (N(CH₃)₂), 0.71 (s, 3H), 0.48 (s, 3H) ((CH₃)₂-Si). ¹³C NMR (pyridine-*d*₅): δ 165.55, 163.17 (NCO), 146.08, 133.38, 131.02, 128.97, 128.72, 128.04, 125.35, 125.13, 124.77, 124.54, 124.47, 123.80, 121.98, 111.67, 108.37, 105.05 (C₉H₆ + C₆H₅), 89.20, 81.00 (C₂B₁₀H₁₀), 36.41, 36.32, 31.02, 28.51 (N(CH₃)₂), -1.66, -1.56 ((CH₃)₂Si). ¹¹B NMR (pyridine-*d*₅): δ -1.1 (3), -5.6 (2), -8.7 (1), -10.8 (4). IR (KBr, cm⁻¹): ν 3057 (w), 3025 (w), 2957 (m), 2923 (m), 2876 (w), 2573 (vs), 1634 (w), 1565 (vs), 1491 (vs), 1445 (vs), 1407 (vs), 1305 (w), 1250 (m), 1212 (m), 1158 (w), 1089 (m), 1032 (w), 929 (w), 833 (m), 804 (s), 749 (m), 697 (m), 645 (m). Anal. Calcd for C₃₁H₄₄B₁₀N₄O₂-SiZr: C, 50.85; H, 6.06; N, 7.65. Found: C, 50.68; H, 6.07; N, 7.51.

Preparation of [η⁵:σ-Me₂Si(C₉H₆)(C₂B₁₀H₁₀)]Zr(η²-OC-(NMe₂)NPh)[η²-OC(NMe₂)N(Ph)C(=NPh)O]·THF (7b**·THF).** To a THF (20 mL) solution of **6b** (184 mg, 0.25 mmol) was added dropwise a THF (10 mL) solution of PhNCO (30 mg, 0.25 mmol) at room temperature with stirring. The mixture was refluxed for 3 h. After removal of the precipitate, the clear yellow solution was concentrated under vacuum to about 10 mL, to which was added a few drops of toluene. **7b**·THF was isolated as colorless crystals after this solution stood at room temperature for 5 days (160 mg, 69%). ¹H NMR (pyridine-*d*₅): δ 7.90 (m, 2H), 7.63 (m, 2H), 7.47–7.37 (m, 8H), 7.33–7.10 (m, 6H), 6.54 (d, *J* = 3.0 Hz, 1H), 6.37 (d, *J* = 3.0 Hz, 1H), 5.89 (d, *J* = 7.8 Hz, 1H) (C₉H₆ + C₆H₅), 3.64 (m, 4H), 1.59 (m, 4H) (THF), 2.58 (s, 9H), 1.88 (s, 3H) (N(CH₃)₂), 0.77 (s, 3H), 0.56 (s, 3H) ((CH₃)₂Si). ¹³C NMR (pyridine-*d*₅): δ 164.70, 160.76, 152.51 (NCO), 146.86, 140.42, 132.38, 132.04, 129.23, 128.88, 128.70, 128.60, 128.12, 128.00, 127.09, 126.51, 125.96, 125.39, 124.84, 124.63, 124.19, 123.75, 121.25, 111.91 (C₉H₆ + C₆H₅), 104.56, 81.41 (C₂B₁₀H₁₀), 67.14, 25.11 (OC₄H₉), 36.28, 36.54, 31.02, 28.51 (N(CH₃)₂), -1.57, -1.70 ((CH₃)₂Si). ¹¹B NMR (pyridine-*d*₅): δ -1.9 (2), -6.1 (3), -10.4 (5). IR (KBr, cm⁻¹): ν 3055 (w), 3019 (w), 2964 (m), 2932 (m), 2872 (m), 2575 (vs), 2540 (vs), 1704 (s), 1636 (vs), 1579 (vs), 1489 (vs), 1438 (vs), 1410 (vs), 1293 (m), 1243 (s), 1209 (m), 1157 (w), 1088 (m), 1062 (m), 1004 (m), 916 (m), 837 (m), 807 (s), 754 (s), 702 (s), 646 (m). Anal. Calcd for C₄₂H₅₇B₁₀N₅O₄SiZr: C, 54.63; H, 6.22; N, 7.59. Found: C, 54.75; H, 6.11; N, 7.68.

Reaction of 7b with Excess PhNCO. **7b**·THF (50 mg, 0.06 mmol) was dissolved in a mixture of THF and toluene (20 mL, 1:1), to which was added PhNCO (360 mg, 3.0 mmol). The mixture was refluxed for 10 h. The resultant brown solution was concentrated under vacuum to about 8 mL and cooled to -20 °C, giving colorless crystals (220 mg, 61%). This product was identified as (PhNCO)₃ by ¹H, ¹³C NMR, MS and unit cell measurement.¹⁸

Preparation of [η⁵:σ-Me₂C(C₉H₆)(C₂B₁₀H₁₀)]Zr(NMe₂)-[η²-SC(NMe₂)NBuⁿ] (8a**).** To a toluene (20 mL) solution of **1a** (240 mg, 0.5 mmol) was added dropwise a toluene (10 mL) solution of *n*-BuNCS (60 mg, 0.5 mmol) at 0 °C with stirring, and the mixture was stirred at room temperature overnight. The clear orange solution was concentrated under vacuum to about 10 mL, to which was added a few drops of *n*-hexane. **8a** was isolated as yellow crystals after this solution stood at room temperature for 1 week (180 mg, 61%). ¹H NMR (pyridine-*d*₅): δ 8.10 (d, *J* = 8.4 Hz, 1H), 7.56 (d, *J* = 7.8 Hz, 1H), 7.14 (m, 2H), 6.78 (d, *J* = 3.6 Hz, 1H), 6.42 (d, *J* = 3.6 Hz, 1H) (C₉H₆), 3.29 (m, 2H) (NCH₂), 2.94 (s, 6H), 2.76 (s, 6H) (N(CH₃)₂), 1.87 (s, 3H), 1.72 (s, 3H) ((CH₃)₂C), 1.25 (m, 4H) ((CH₂)₂), 0.92 (t, *J* = 6.9 Hz, 3H) (CH₂CH₃). ¹³C NMR (pyridine-*d*₅): δ 175.60 (NCS), 135.76, 128.72, 127.98, 126.55, 125.14, 124.53, 121.71, 118.00, 104.62 (C₉H₆), 95.42 (C₂B₁₀H₁₀), 50.72 (NCH₂), 40.18, 32.36, 32.08 (N(CH₃)₂), 44.40, 28.52, 20.11 ((CH₃)₂C), 35.33, 31.02, 13.55 ((CH₂)₂CH₃). ¹¹B NMR (pyridine-

(18) Zhou, X.; Zhang, L.; Zhu, M.; Cai, R.; Weng, L.; Huang, Z.; Wu, Q. *Organometallics* **2001**, *20*, 5700.

Table 1. Crystal Data and Summary of Data Collection and Refinement for 2a, 3a, 4a,b, and 5a,b

	2a	3a ·C ₆ H ₅ CH ₃	4a ·2C ₆ H ₅ CH ₃	4b ·2THF	5a ·2C ₆ H ₅ CH ₃	5b
formula	C ₃₂ H ₄₄ B ₁₀ N ₄ Zr	C ₃₁ H ₄₈ B ₁₀ N ₄ Zr	C ₄₆ H ₇₂ B ₂₀ O ₄ Zr ₂	C ₃₈ H ₇₂ B ₂₀ O ₆ Si ₂ Zr ₂	C ₃₄ H ₅₀ B ₁₀ N ₂ S ₄ Zr	C ₁₉ H ₃₄ B ₁₀ N ₂ S ₄ SiZr
cryst size (mm)	0.52 × 0.27 × 0.21	0.36 × 0.30 × 0.13	0.22 × 0.20 × 0.16	0.40 × 0.20 × 0.10	0.45 × 0.18 × 0.15	0.40 × 0.32 × 0.18
fw	684.03	676.05	1087.68	1079.78	814.32	646.13
cryst syst	triclinic	triclinic	monoclinic	monoclinic	monoclinic	monoclinic
space group	<i>P</i> <i>1</i>	<i>P</i> <i>1</i>	<i>P</i> <i>2</i> ₁ / <i>n</i>	<i>P</i> <i>2</i> ₁ / <i>n</i>	<i>P</i> <i>2</i> ₁ / <i>n</i>	<i>P</i> <i>2</i> ₁ / <i>n</i>
<i>a</i> , Å	9.019(1)	10.780(2)	11.011(2)	11.154(2)	11.556(1)	10.738(1)
<i>b</i> , Å	12.899(1)	11.251(3)	12.093(1)	12.477(3)	12.393(1)	16.778(1)
<i>c</i> , Å	16.468(1)	16.684(3)	20.825(4)	20.636(4)	29.481(3)	18.912(1)
α, deg	72.58(1)	92.23(1)	90	90	90	90
β, deg	79.59(1)	91.93(1)	91.27(1)	91.12(3)	102.29(1)	94.11(1)
γ, deg	82.20(1)	116.22(2)	90	90	90	90
<i>V</i> , Å ³	1790.9(2)	1811.0(7)	2772.3(8)	2871(1)	4125.3(7)	3398.4(4)
<i>Z</i>	2	2	2	2	4	4
<i>D</i> _{calcd} , Mg/m ³	1.268	1.240	1.303	1.249	1.311	1.263
radiation (λ), Å				Mo Kα (0.710 73)		
2θ range, deg	2.6–56.0	4.2–50.0	4.0–50.0	3.8–50.0	3.6–52.0	4.2–51.0
μ, mm ^{−1}	0.336	0.331	0.417	0.444	0.497	0.618
<i>F</i> (000)	708	704	1120	1112	1688	1320
no. of obsd rflns	8483	4268	2929	3289	5604	5281
no. of params refnd	425	386	318	318	425	335
goodness of fit	0.961	1.066	1.095	1.073	1.100	1.091
<i>R</i> 1	0.044	0.089	0.074	0.088	0.067	0.066
<i>wR</i> 2	0.087	0.237	0.163	0.238	0.177	0.174

Table 2. Crystal Data and Summary of Data Collection and Refinement for 6a,b, 7b, 8a,b and 9a

	6a	6b	7b ·THF	8a	8b	9a
formula	C ₃₂ H ₄₄ B ₁₀ N ₄ O ₂ Zr	C ₃₁ H ₄₄ B ₁₀ N ₄ O ₂ SiZr	C ₄₂ H ₅₇ B ₁₀ N ₅ O ₄ SiZr	C ₂₃ H ₄₃ B ₁₀ N ₃ SSZr	C ₂₂ H ₄₃ B ₁₀ N ₃ SSiZr	C ₂₈ H ₅₂ B ₁₀ N ₄ S ₂ Zr
cryst size (mm)	0.45 × 0.22 × 0.12	0.50 × 0.50 × 0.21	0.40 × 0.36 × 0.14	0.75 × 0.35 × 0.34	0.38 × 0.25 × 0.20	0.24 × 0.12 × 0.10
fw	716.03	732.11	923.34	592.98	609.06	708.18
cryst syst	monoclinic	monoclinic	triclinic	monoclinic	monoclinic	triclinic
space group	<i>P</i> <i>2</i> ₁ / <i>n</i>	<i>P</i> <i>2</i> ₁ / <i>n</i>	<i>P</i> <i>1</i>	<i>P</i> <i>2</i> ₁ / <i>c</i>	<i>P</i> <i>2</i> ₁ / <i>n</i>	<i>P</i> <i>1</i>
<i>a</i> , Å	11.333(2)	11.455(3)	12.708(3)	12.738(1)	8.213(2)	11.747(1)
<i>b</i> , Å	17.457(4)	17.546(4)	14.300(3)	16.624(1)	21.496(4)	11.956(1)
<i>c</i> , Å	18.333(4)	18.394(4)	14.366(3)	15.883(1)	17.806(4)	16.297(1)
α, deg	90	90	70.15(3)	90	90	98.57(1)
β, deg	92.14(3)	92.71(1)	78.06(3)	113.16(1)	93.21(3)	97.99(1)
γ, deg	90	90	79.28(3)	90	90	107.33(1)
<i>V</i> , Å ³	3624(1)	3692(1)	2383.3(8)	3092.3(5)	3139(1)	2119.3(3)
<i>Z</i>	4	4	2	4	4	2
<i>D</i> _{calcd} , Mg/m ³	1.312	1.317	1.288	1.274	1.289	1.110
radiation (λ), Å				Mo Kα (0.710 73)		
2θ range, deg	3.2–50.0	3.2–56.0	3.0–51.0	3.4–56.0	3.0–50.0	4.0–50.0
μ, mm ^{−1}	0.339	0.365	0.302	0.442	0.474	0.381
<i>F</i> (000)	1480	1512	962	1232	1264	740
no. of obsd rflns	5372	8944	6923	7433	4529	6612
no. of params refnd	452	443	569	354	358	402
goodness of fit	1.071	0.965	1.033	1.041	1.123	0.975
<i>R</i> 1	0.073	0.038	0.077	0.035	0.066	0.081
<i>wR</i> 2	0.178	0.086	0.206	0.102	0.152	0.205

Table 3. Summary of Key Structural Data

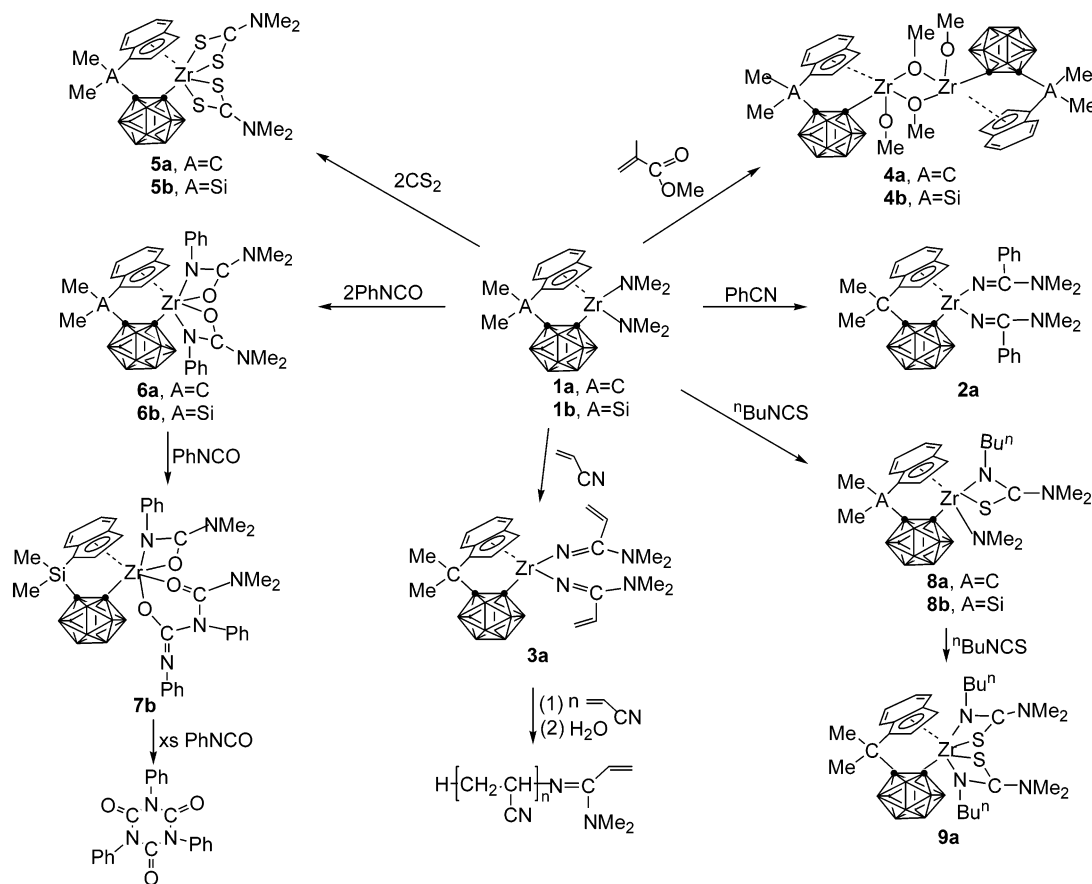
compd	av Zr–C(C ₅ ring) (Å)	Zr–C(cage) (Å)	av Zr–N (Å)	av Zr–O (Å)	av Zr–S (Å)	C(C ₅ ring)–A–C(cage) (deg)	Cent–Zr–C(cage) (deg) ^a
1a^b	2.521(8)	2.326(7)	2.016(8)			109.4(6)	101.6
1b^b	2.541(5)	2.348(5)	2.019(4)			104.8(2)	109.9
2a	2.544(2)	2.359(2)	1.972(2)			110.4(2)	100.4
3a	2.549(8)	2.365(7)	1.974(7)			110.7(6)	100.4
4a	2.539(1)	2.407(10)		1.880(6)		109.7(9)	98.8
				2.159(6) ^c			
4b	2.552(3)	2.448(3)		1.874(2)		103.7(1)	106.3
				2.178(2) ^c			
5a	2.539(2)	2.388(3)			2.638(1)	109.7(2)	99.4
5b	2.558(5)	2.456(5)			2.645(1)	103.7(2)	106.2
6a	2.541(4)	2.378(4)	2.242(3)	2.165(3)		109.5(3)	98.5
6b	2.554(3)	2.414(2)	2.227(2)	2.161(2)		104.3(1)	105.6
7b	2.563(5)	2.422(5)	2.180(4)	2.151(3)		104.3(2)	105.7
8a	2.532(2)	2.410(2)	1.997(2)		2.621(1)	110.1(2)	100.1
			2.268(2) ^d				
8b	2.571(6)	2.438(5)	1.975(5)		2.606(2)	105.8(3)	107.3
			2.270(5) ^d				
9a	2.559(10)	2.398(9)	2.268(8) ^d		2.578(3)	110.5(8)	98.3

^a Cent = centroid of the five-membered ring of the indenyl group. ^b See ref 16. ^c Zr–O(μ) distance. ^d Zr–N(imido) distance.

*d*₅): δ −5.3 (2), −7.0 (2), −11.4 (6). IR (KBr, cm^{−1}): ν 3023 (w), 2954 (s), 2922 (m), 2879 (s), 2596 (vs), 2552 (vs), 1545 (vs), 1457 (s), 1427 (m), 1349 (s), 1255 (w), 1212 (w), 1152 (m), 1122 (m), 1053 (m), 917 (m), 797 (m), 741 (m), 657 (w), 547 (m). Anal. Calcd for C₂₃H₄₃B₁₀N₃SSZr: C, 46.58; H, 7.31; N, 7.09. Found: C, 46.81; H, 7.33; N, 6.93.

Preparation of [η⁵:σ-Me₂Si(C₉H₆)(C₂B₁₀H₁₀)]Zr(NMe₂)-[η²:SC(NMe₂)NBU^q] (8b). This compound was prepared as yellow crystals from **1b** (247 mg, 0.5 mmol) and *n*-BuNCS (60 mg, 0.5 mmol) using a procedure identical with that reported for **8a**. Yield: 230 mg (75%). ¹H NMR (pyridine-*d*₅): δ 7.92 (d, *J* = 7.8 Hz, 1H), 7.68 (d, *J* = 7.8 Hz, 1H), 7.23 (m, 1H), 7.20

Scheme 1



(m, 1H), 6.92 (d, $J = 3.3$ Hz, 1H), 6.79 (d, $J = 3.3$ Hz, 1H) (C_9H_6), 3.30 (m, 2H) (NCH_2), 3.00 (s, 6H), 2.78 (s, 6H) ($\text{N}(\text{CH}_3)_2$), 1.24 (m, 4H) ($(\text{CH}_2)_2$), 0.91 (t, $J = 6.3$ Hz, 3H) (CH_2CH_3), 0.73 (s, 3H), 0.58 (s, 3H) ($(\text{CH}_3)_2\text{Si}$). ^{13}C NMR (pyridine- d_5): δ 174.91 (NCS), 131.39, 129.11, 127.99, 125.55, 125.49, 124.69, 123.79, 110.08, 104.28 (C_9H_6), 100.14, 82.56 ($\text{C}_2\text{B}_{10}\text{H}_{10}$), 50.96 (NCH_2), 39.95, 32.03, 20.11 ($\text{N}(\text{CH}_3)_2$), 31.04, 22.18, 13.50 ($(\text{CH}_2)_2\text{CH}_3$), -0.91, -1.76 ($(\text{CH}_3)_2\text{Si}$). ^{11}B NMR (pyridine- d_5): δ -1.6 (2), -5.0 (2), -10.1 (6). IR (KBr, cm^{-1}): ν 3034 (w), 2955 (s), 2900 (s), 2779 (m), 2572 (vs), 1538 (vs), 1453 (m), 1422 (m), 1345 (s), 1299 (w), 1255 (s), 1149 (s), 1119 (s), 1090 (s), 1057 (m), 972 (w), 911 (s), 833 (s), 806 (s), 745 (m), 680 (m), 545 (m). Anal. Calcd for $\text{C}_{22}\text{H}_{43}\text{B}_{10}\text{N}_3\text{SSiZr}$: C, 43.38; H, 7.12; N, 6.90. Found: C, 43.30; H, 6.90; N, 7.06.

Preparation of $[\eta^5\text{-}\sigma\text{-Me}_2\text{C}(\text{C}_9\text{H}_6)(\text{C}_2\text{B}_{10}\text{H}_{10})]\text{Zr}[\eta^2\text{-SC}(\text{NMe}_2)\text{NBu}^n]_2$ (9a**).** Compound **8a** (300 mg, 0.5 mmol) was dissolved in a mixture of THF and toluene (20 mL, 1:1), to which was added $n\text{-BuNCS}$ (60 mg, 0.5 mmol) in THF (10 mL). The reaction mixture was then refluxed for 10 h. The resulting clear orange solution was concentrated under vacuum to about 10 mL, to which was added a few drops of n -hexane. **9a** was isolated as pale yellow crystals after this solution stood at room temperature for 3 days (270 mg, 76%). ^1H NMR (pyridine- d_5): δ 8.22 (d, $J = 8.7$ Hz, 1H), 7.69 (d, $J = 8.4$ Hz, 1H), 7.44 (dd, $J = 6.6$ and 8.4 Hz, 1H), 7.31 (m, 1H), 7.13 (d, $J = 3.3$ Hz, 1H), 6.13 (d, $J = 3.3$ Hz, 1H) (C_9H_6), 4.44 (m, 2H), 3.49 (m, 2H) (NCH_2), 3.04 (s, 6H), 2.78 (s, 6H) ($\text{N}(\text{CH}_3)_2$), 1.88 (s, 3H), 1.73 (s, 3H) ($(\text{CH}_3)_2\text{C}$), 1.48 (m, 4H), 1.31–1.23 (m, 4H) ($(\text{CH}_2)_2$), 0.91–0.80 (m, 6H) (CH_2CH_3). ^{13}C NMR (pyridine- d_5): δ 176.62, 171.65 (NCS), 133.31, 128.71, 127.97, 126.23, 125.06, 123.60, 123.30, 119.51, 117.65 (C_9H_6), 104.73, 97.33 ($\text{C}_2\text{B}_{10}\text{H}_{10}$), 51.78, 51.32 (NCH_2), 40.13, 40.05, 39.77, 39.49 ($\text{N}(\text{CH}_3)_2$), 43.62, 22.14, 20.28 ($(\text{CH}_3)_2\text{C}$), 34.66, 32.80, 31.65, 31.01 ($(\text{CH}_2)_2$), 13.54, 13.34 (CH_2CH_3). ^{11}B NMR (pyridine- d_5): δ -5.6 (2), -7.2

(2), -10.9 (6). IR (KBr, cm^{-1}): ν 3039 (w), 2955 (s), 2928 (s), 2870 (m), 2807 (w), 2592 (vs), 2549 (vs), 1545 (vs), 1455 (m), 1344 (s), 1244 (w), 1212 (w), 1119 (vs), 1052 (m), 1023 (w), 805 (m), 738 (s), 658 (w), 557 (w). Anal. Calcd for $\text{C}_{28}\text{H}_{52}\text{B}_{10}\text{N}_4\text{S}_2\text{-Zr}$: C, 47.48; H, 7.40; N, 7.91. Found: C, 47.36; H, 7.60; N, 7.77.

X-ray Structure Determination. All single crystals were immersed in Paratone-N oil and sealed under N_2 in thin-walled glass capillaries. Data were collected at 293 K on an MSC/Rigaku RAXIS-IIC imaging plate using Mo $\text{K}\alpha$ radiation from a Rigaku rotating-anode X-ray generator operating at 50 kV and 90 mA or on a Bruker SMART 1000 CCD diffractometer using Mo $\text{K}\alpha$ radiation. An empirical absorption correction was applied using the SADABS program.¹⁹ All structures were solved by direct methods and subsequent Fourier difference techniques and refined anisotropically for all non-hydrogen atoms by full-matrix least-squares calculations on F^2 using the SHELXTL program package (PC version).²⁰ Most of the carborane hydrogen atoms were located from difference Fourier syntheses. All other hydrogen atoms were geometrically fixed using the riding model. Crystal data and details of data collection and structure refinement are given in Tables 1 and 2, respectively. Key structural parameters are listed in Table 3. Further details are included in the Supporting Information.

Results

Reaction with PhCN. $[\eta^5\text{-}\sigma\text{-Me}_2\text{C}(\text{C}_9\text{H}_6)(\text{C}_2\text{B}_{10}\text{H}_{10})]\text{-Zr}(\text{NMe}_2)_2$ (**1a**) reacted readily with 2 equiv of PhCN to

(19) Sheldrick, G. M. SADABS: Program for Empirical Absorption Correction of Area Detector Data; University of Göttingen, Göttingen, Germany, 1996.

(20) SHELXTL V 5.03 Program Package; Siemens Analytical X-ray Instruments, Inc., Madison, WI, 1995.

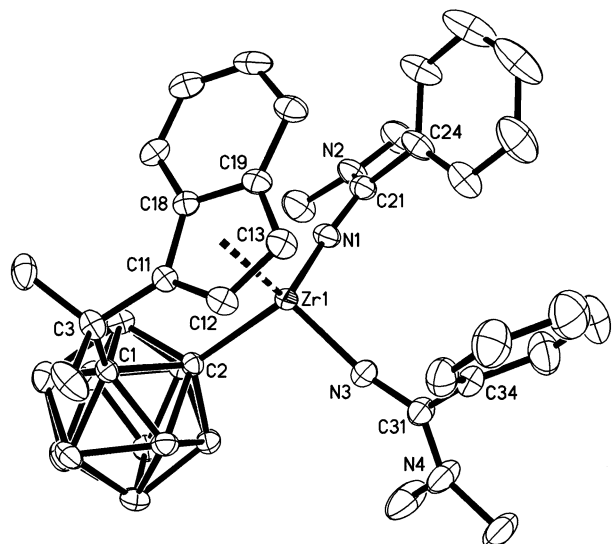


Figure 1. Molecular structure of $[\eta^5:\sigma\text{-Me}_2\text{C}(\text{C}_9\text{H}_6)(\text{C}_2\text{B}_{10}\text{H}_{10})]\text{Zr}[\text{N}=\text{C}(\text{Ph})\text{NMe}_2]_2$ (**2a**; thermal ellipsoids drawn at the 35% probability level).

give the diinsertion product $[\eta^5:\sigma\text{-Me}_2\text{C}(\text{C}_9\text{H}_6)(\text{C}_2\text{B}_{10}\text{H}_{10})]\text{Zr}[\text{N}=\text{C}(\text{Ph})\text{NMe}_2]_2$ (**2a**) (Scheme 1). **2a** did not react further with excess PhCN. Both mono- and diinsertion products were detected by NMR when 1 equiv of PhCN was added to **1a**. Attempts to isolate pure monoininsertion product from the reaction mixture were unsuccessful.

The X-ray structural analysis of **2a** confirms that the $\text{C}\equiv\text{N}$ triple bond of PhCN inserts into the Zr–N bond or the NMe_2 group migrates to the carbon position of the CN unit, leading to the formation of **2a**. The Zr atom is η^5 -bound to the five-membered ring of the indenyl group and σ -bound to a cage carbon atom and two nitrogen atoms in a distorted-tetrahedral geometry, shown in Figure 1. The structural parameters of the $[\eta^5:\sigma\text{-Me}_2\text{C}(\text{C}_9\text{H}_6)(\text{C}_2\text{B}_{10}\text{H}_{10})]\text{Zr}$ fragment are very close to those observed in its parent compound **1a** (Table 3).¹⁶ The average Zr–N distance of 1.972(2) Å is slightly shorter than that of 2.016(8) Å observed in **1a**.¹⁶ The relatively short Zr–N(1,3) distances and the large Zr–N(1,3)–C angles (160.7(2) and 164.0(2)°) indicate partial $\text{N}(\text{p}_\pi)\rightarrow\text{Zr}(\text{d}_\pi)$ interactions between the imido nitrogen and zirconium atoms. In addition, the C–NMe₂ distances (1.358(3) and 1.353(4) Å) are between the N–C single- and double-bond distances, which suggests some degree of $\text{p}-\pi$ bonding in the $\text{N}=\text{CNMe}_2$ moieties. This bonding feature is consistent with the fact that the sums of the C–N–C bond angles around the NMe₂ groups are near 360°.

Reaction with $\text{CH}_2=\text{CHCN}$. It was reported that $\text{M}(\text{NMe}_2)_4$ (M = Ti, Zr, Hf) can initiate the polymerization of $\text{CH}_2=\text{CHCN}$ in the absence of any cocatalysts.^{8a} Although both $(\text{Me}_2\text{N})_3\text{M}[\text{N}=\text{C}(\text{NMe}_2)\text{C}=\text{CH}_2]$ and $(\text{Me}_2\text{N})_3\text{M}[\text{N}=\text{C}=\text{CHCH}_2\text{NMe}_2]$ were suggested to be the first insertion products, neither of these compounds were characterized.²¹ Under similar reaction conditions, **1a** reacted with 2 equiv of $\text{CH}_2=\text{CHCN}$ to generate the diinsertion product $[\eta^5:\sigma\text{-Me}_2\text{C}(\text{C}_9\text{H}_6)(\text{C}_2\text{B}_{10}\text{H}_{10})]\text{Zr}[\text{N}=\text{C}(\text{C}_2\text{H}_3)\text{NMe}_2]_2$ (**3a**). It reacted further with excess $\text{CH}_2=\text{CHCN}$, producing polyacrylonitrile. These results

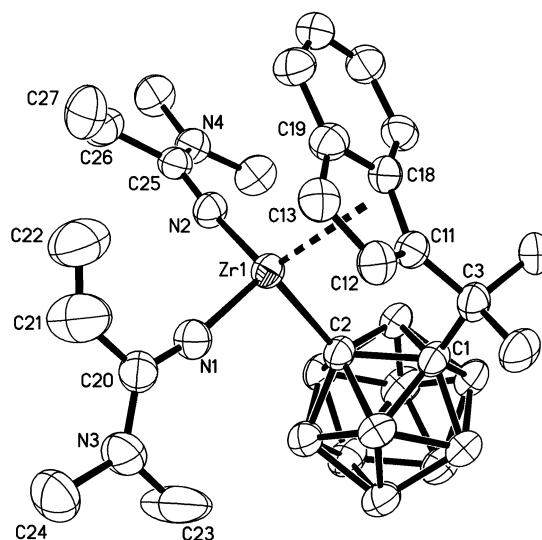


Figure 2. Molecular structure of $[\eta^5:\sigma\text{-Me}_2\text{C}(\text{C}_9\text{H}_6)(\text{C}_2\text{B}_{10}\text{H}_{10})]\text{Zr}[\text{N}=\text{C}(\text{C}_2\text{H}_3)\text{NMe}_2]_2$ (**3a**; thermal ellipsoids drawn at the 35% probability level).

imply that the first 2 equiv of acrylonitrile molecules insert into the Zr–N bond via the CN triple bond to form the intermediate **3a**, and 1 equiv of $\text{CH}_2=\text{CHCN}$ then inserts into the newly formed Zr–N(imido) bond through its C=C double bond to generate the active species containing the Zr–C σ bond, which initiates the chain propagation.

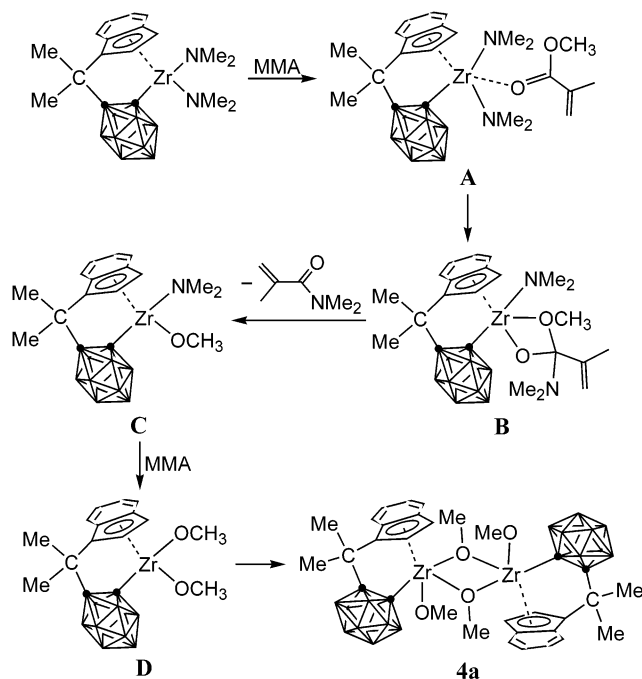
The molecular structure of **3a** has been confirmed by single-crystal X-ray analyses, shown in Figure 2. The asymmetric unit contains one toluene of solvation. The coordination geometry of the Zr atom in **3a** is very close to that in **2a** (Table 3). Similarly, both partial $\text{N}(\text{p}_\pi)\rightarrow\text{Zr}(\text{d}_\pi)$ interactions and some degree of $\text{p}-\pi$ bonding in the $\text{N}=\text{C}-\text{NMe}_2$ moieties are observed in **3a**.

Reaction with $\text{CH}_2=\text{C}(\text{Me})\text{COOMe}$. The C=C double bond in MMA is also activated. It might be anticipated that **1a,b** could initiate the polymerization of MMA. In fact, reaction of **1a,b** with excess MMA did not produce any polymeric materials. On the other hand, stoichiometric reactions gave the zirconium methoxide compounds $[\{\eta^5:\sigma\text{-Me}_2\text{A}(\text{C}_9\text{H}_6)(\text{C}_2\text{B}_{10}\text{H}_{10})\}\text{Zr}(\text{OCH}_3)(\mu\text{-OCH}_3)]_2$ (A = C (**4a**), Si (**4b**)) in about 80% isolated yield (Scheme 1). In the reaction mixture, $\text{CH}_2=\text{C}(\text{Me})\text{CONMe}_2$ was also detected by ¹H NMR and GC-MS spectroscopy. On the basis of these experimental results, a possible reaction pathway is proposed in Scheme 2. Coordination of MMA and migration of NMe₂ give the insertion product **B**. Elimination of $\text{CH}_2=\text{C}(\text{Me})\text{CONMe}_2$ generates the exchange product **C**. Repeat of the above reactions yields the monomer **D**, which dimerizes to afford the final product **4a**. The oxophilicity of Zr(IV) is probably the driving force for the reactions.

The molecular structures of **4a,b** are confirmed by X-ray crystallographic analyses, which indicate that these compounds are isostructural and isomorphous. They are centrosymmetric dimers and show either two toluene (for **4a**) or two THF molecules of solvation (for **4b**). Figure 3 shows their representative structure. Each Zr atom is η^5 -bound to the five-membered ring of the indenyl group and σ -bound to a cage carbon atom and one terminal methoxy and two doubly bridging methoxy groups, thus affording a distorted-square-pyramidal

(21) Jenkins, A. D.; Lappert, M. F.; Srivastava, R. C. *Eur. Polym. J.* **1971**, *7*, 289.

Scheme 2



geometry. As indicated in Table 3, both the average Zr–C(C₅ ring) and Zr–C(cage) distances are slightly longer than those in their parent compounds **1a,b**, due to the increased steric hindrance. As expected, the Zr–O(terminal) distances are significantly shorter than the Zr–O(bridging) ones. The short Zr–O(terminal) distances and very large Zr–O–C angles (170.3(7) and 171.9(3)°) indicate partial O(p_π)→Zr(d_π) interactions between Zr(IV) and the terminal MeO group.²²

Reaction with CS₂. Reactions of **1a,b** with CS₂ were fast, and no monoinsertion products were isolated in equimolar reactions. Only the diinsertion products [η^5 : σ -Me₂A(C₉H₆)(C₂B₁₀H₁₀)]Zr(η^2 -S₂CNMe₂)₂ (A = C (**5a**), Si (**5b**)) were obtained in high yield. Both **1a** and **1b** also reacted with CO₂, as indicated by NMR. Attempts to isolate pure insertion products, however, failed.

Compounds **5a,b** are isostructural, and their molecular structures are shown in Figure 4. The crystal lattice of **5a** contains two independent toluene molecules of solvation, whereas that for **5b** is unsolvated. It is clear that CS₂ inserts into the Zr–N bond to form the η^2 -S₂-CNMe₂ moiety. The small differences in the C–S distances (0.010 and 0.027 Å in **5a**, 0.022 and 0.041 Å in **5b**) suggest that the negative charge is delocalized over the S–C–S fragment. Some degree of p– π bonding in the S=CNMe₂ moieties is also observed in the present compounds.

Reaction with PhNCO. Only the diinsertion products [η^5 : σ -Me₂A(C₉H₆)(C₂B₁₀H₁₀)]Zr(η^2 -OC(NMe₂)NPh)₂ (A = C (**6a**), Si (**6b**)) were isolated from either 1:1 or 1:2 molar ratio reactions. The C=O double bond of the PhN=C=O molecule inserts into the Zr–N bond to form the η^2 -OC(NMe₂)NPh moiety with some electronic delocalization over the O–C–N unit. The third equivalent of the PhN=C=O molecule can further insert into the newly formed Zr–N bond to generate the triinsertion product [η^5 : σ -Me₂Si(C₉H₆)(C₂B₁₀H₁₀)]Zr(η^2 -OC(NMe₂)-

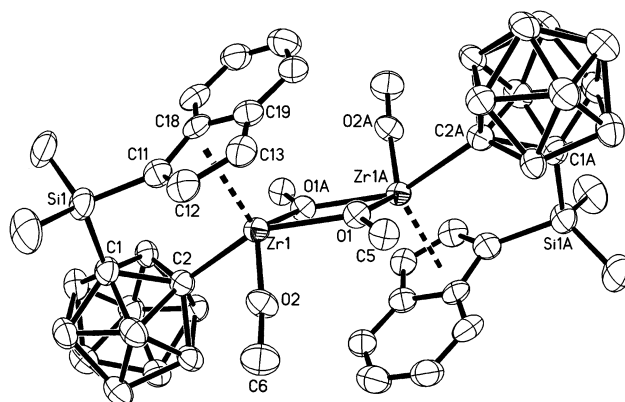


Figure 3. Molecular structure of [η^5 : σ -Me₂Si(C₉H₆)-(C₂B₁₀H₁₀)]Zr(OCH₃)(μ -OCH₃)₂ (**4b**; thermal ellipsoids drawn at the 35% probability level).

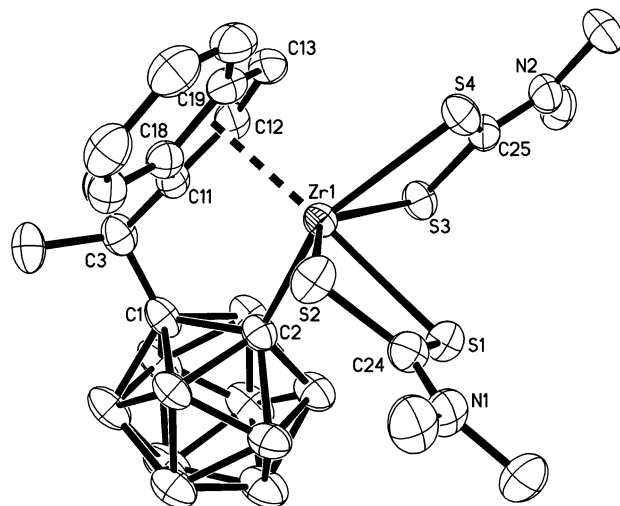


Figure 4. Molecular structure of [η^5 : σ -Me₂C(C₉H₆)-(C₂B₁₀H₁₀)]Zr(η^2 -S₂CNMe₂)₂ (**5a**; thermal ellipsoids drawn at the 35% probability level).

NPh][η^2 -OC(NMe₂)N(Ph)C(=NPh)O] (**7b**) (Scheme 1). A tetrainsertion product was not detected by NMR from the reaction of **7b** with 1 equiv of PhN=C=O; instead, the trimer (PhNCO)₃ was isolated and identified. In fact, either **7b** or **1b** can catalyze the trimerization of PhN=C=O. These results suggest that the fourth equivalent of isocyanate is superior in reacting with the coordinated η^2 -OC(NMe₂)N(Ph)C(=NPh)O moiety, leading to the formation of trimer, probably because of steric reasons. The proposed catalytic cycle is shown in Scheme 3.

Polymerization of isocyanates catalyzed by (η^5 -Me-C₅H₄)₂YNPr_i₂(THF)²³ and (η^5 -C₅H₅)TiCl₂(NMe₂)²⁴ were reported. The presence of a carboranyl unit in **1b** might be responsible for the differences in their reactivities.

Single-crystal X-ray analyses reveal that compounds **6a,b** are isostructural and isomorphous. Figure 5 shows a representative structure. The geometry of the [η^5 : σ -Me₂A(C₉H₆)(C₂B₁₀H₁₀)]Zr fragment is almost identical with that observed in this family of compounds. The structural parameters of the η^2 -OC(NMe₂)NPh moieties indicate some electronic delocalization over the O–C–N unit.

(22) McGeary, M. J.; Coan, P. S.; Folting, K.; Streib, W. E.; Caulton, K. G. *Inorg. Chem.* **1989**, *28*, 3283.

(23) Mao, L.; Shen, Q.; Xue, M.; Sun, J. *Organometallics* **1997**, *16*, 3711.

(24) Patten, T. E.; Novak, B. M. *Macromolecules* **1993**, *26*, 436.

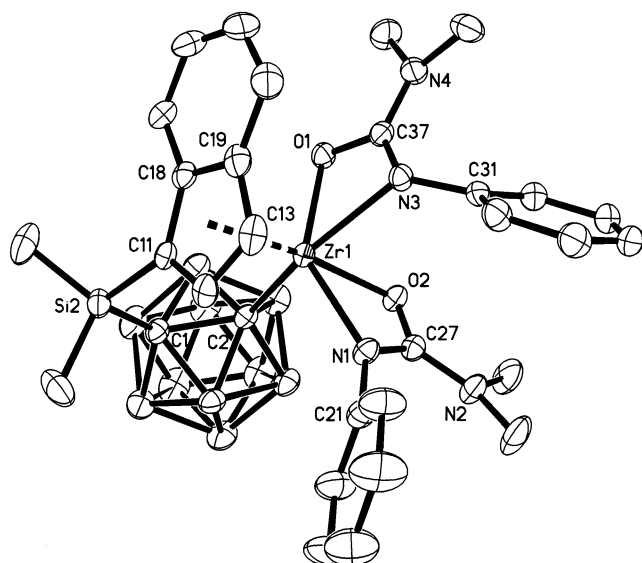
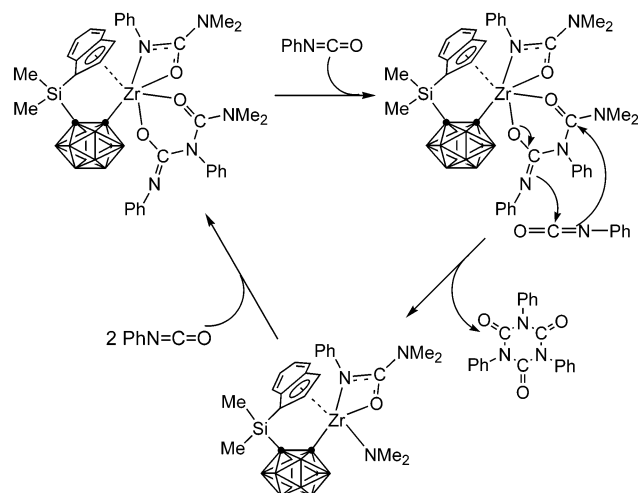


Figure 5. Molecular structure of $[\eta^5:\sigma\text{-Me}_2\text{Si}(\text{C}_9\text{H}_6)\text{-(C}_2\text{B}_{10}\text{H}_{10})]\text{Zr}[\eta^2\text{-OC(NMe}_2\text{)NPh}]_2$ (**6b**; thermal ellipsoids drawn at the 35% probability level).

Scheme 3



The molecular structure of **7b** is shown in Figure 6. Its crystal lattice contains a molecule of THF. The structural parameters indicate that there is some electronic delocalization over the O(2)–C(27)–N(1), O(1)–C(37)–N(3), and O(3)–C(4)–N(5) units. Space-filling drawings of **7b** show that the central Zr atom is fully protected by the surrounding ligands and no coordination sites are available for the coordination of the fourth equivalent of isocyanate, which could explain why no further insertion was observed.

Reaction with ⁿBuNCS. Reactions of **1a,b** with 1 equiv of ⁿBuNCS gave the monoinsertion products $[\eta^5:\sigma\text{-Me}_2\text{A}(\text{C}_9\text{H}_6)(\text{C}_2\text{B}_{10}\text{H}_{10})]\text{Zr}(\text{NMe}_2)[\eta^2\text{-SC(NMe}_2\text{)NBu}^n]$ (A = C (**8a**), Si (**8b**)). **8a** reacted further with the second equivalent of ⁿBuNCS, affording the diinsertion derivative $[\eta^5:\sigma\text{-Me}_2\text{C}(\text{C}_9\text{H}_6)(\text{C}_2\text{B}_{10}\text{H}_{10})]\text{Zr}[\eta^2\text{-SC(NMe}_2\text{)NBu}^n]_2$ (**9a**). **9a** did not react further with ⁿBuNCS, which is different from the case for **6a**.

Compounds **8a,b** are isostructural, but not isomorphous. Figure 7 shows a representative molecular structure. The Zr–N(amido) distance is much longer than the Zr–N(imido) distance by ca. 0.27 Å in **8a** and 0.29 Å in **8b**, respectively. The Zr–S distances are

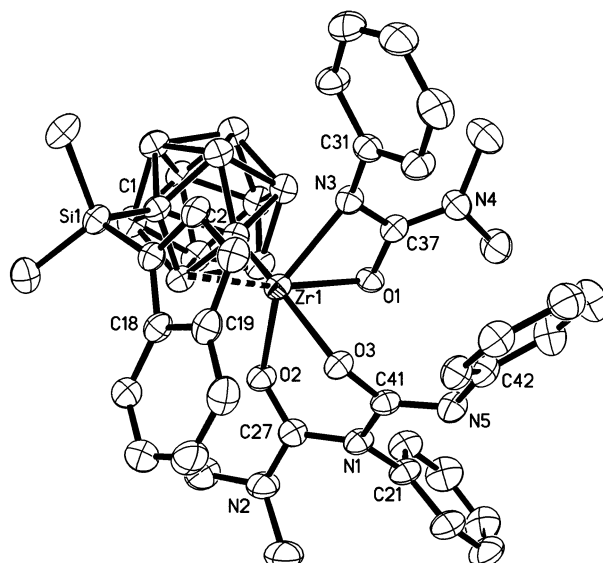


Figure 6. Molecular structure of $[\eta^5:\sigma\text{-Me}_2\text{Si}(\text{C}_9\text{H}_6)\text{-(C}_2\text{B}_{10}\text{H}_{10})]\text{Zr}[\eta^2\text{-OC(NMe}_2\text{)NPh}][\eta^2\text{-OC(NMe}_2\text{)N(Ph)C(=NPh)O}]$ (**7b**; thermal ellipsoids drawn at the 35% probability level).

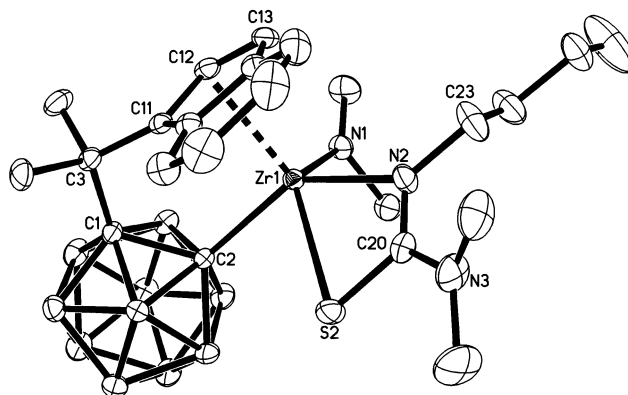


Figure 7. Molecular structure of $[\eta^5:\sigma\text{-Me}_2\text{C}(\text{C}_9\text{H}_6)\text{-(C}_2\text{B}_{10}\text{H}_{10})]\text{Zr}(\text{NMe}_2)[\eta^2\text{-SC(NMe}_2\text{)NBu}^n]$ (**8a**; thermal ellipsoids drawn at the 35% probability level).

comparable to those found in **5a,b**. Some degree of p–π bonding in the N–C–S moiety is observed in the present compounds.

The molecular structure of **9a** is shown in Figure 8. Its structural parameters are similar to those of its parent compound **8a**. Some degree of p–π bonding in both N–C–S moieties is also observed.

Discussion

The above experimental results show that the unsaturated molecules insert exclusively into the Zr–N bonds of **1a,b** and the Zr–C(cage) bond remains intact. The proposed reaction pathway is that coordination of the unsaturated molecule followed by nucleophilic attack initiates the insertion, into either the Zr–N (route a) or the Zr–C(cage) (route b) bond, which is most probably governed by steric factors,^{10b,25} shown in Scheme 4. To help understand the experimental results, the space-filling drawings of **1a** are generated using X-ray data¹⁶ and shown in parts a and b of Figure 9, respectively.

(25) Gambarotta, S.; Strologo, S.; Floriani, C.; Chiesi-Villa, A.; Guastini, C. *Inorg. Chem.* **1985**, *24*, 654.

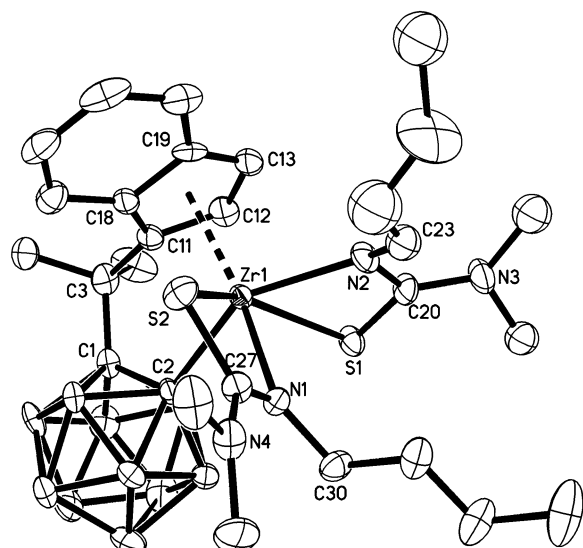
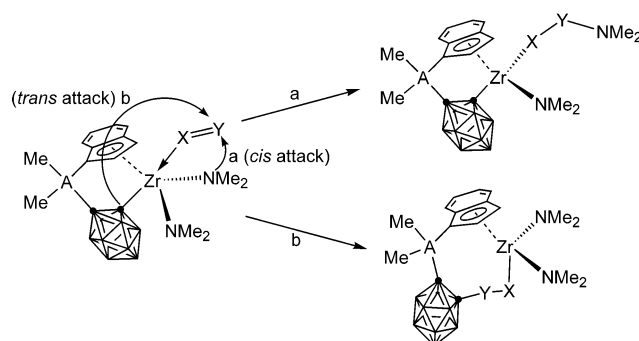


Figure 8. Molecular structure of $[\eta^5:\sigma\text{-Me}_2\text{C}(\text{C}_9\text{H}_6)\text{-(C}_2\text{B}_{10}\text{H}_{10})]\text{Zr}[\eta^2\text{-SC}(\text{NMe}_2)\text{NBU}]_2$ (**9a**; thermal ellipsoids drawn at the 35% probability level).

These figures clearly show that two NMe_2 groups and the five-membered ring form the largest open area around the central Zr atom for the coordination of an unsaturated molecule. Thus, the unsaturated substrate can only coordinate to the Zr metal in a position that is trans to the carboranyl group, which probably prevents the migration of the cage (route b in Scheme 4) and

Scheme 4



makes the insertion into the Zr-N bond as the only possible pathway (route a in Scheme 4). The general lack of mobility of the linked carboranyl moiety may also prevent such a trans attack.

After the insertion of the first molecule, although the coordination environment of the Zr atom becomes more crowded, the largest open site available for the coordination of an unsaturated molecule is still the triangular area generated by the amido and imido nitrogen atoms (N1 and N2) and the five-membered ring, as illustrated by the space-filling drawings of **8a** (Figures 10). An attack trans to the carboranyl ligand is again preferred for the second equivalent of unsaturated molecule. Whether or not the third equivalent of unsaturated molecule is inserted into the newly formed Zr-N bond

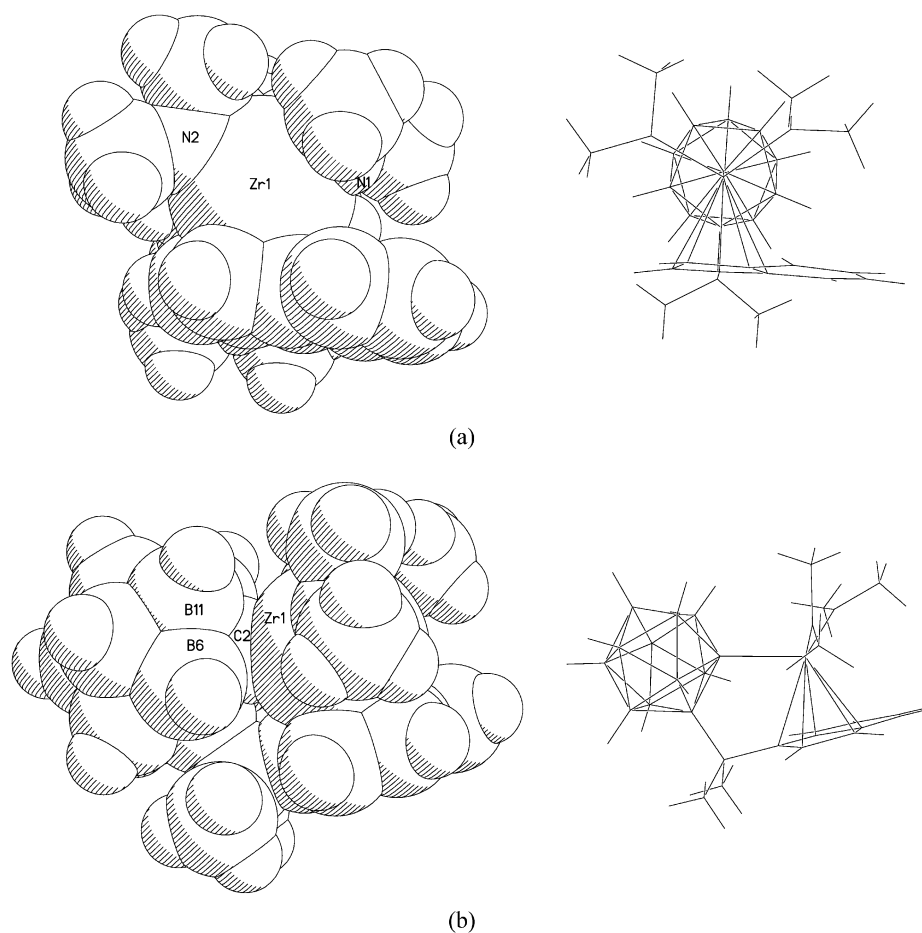


Figure 9. Space-filling drawings of $[\eta^5:\sigma\text{-Me}_2\text{C}(\text{C}_9\text{H}_6)(\text{C}_2\text{B}_{10}\text{H}_{10})]\text{Zr}(\text{NMe}_2)_2$ (**1a**):¹⁶ (a) axial view along the $\text{Zr-C}(\text{cage})$ bond; (b) equatorial view.

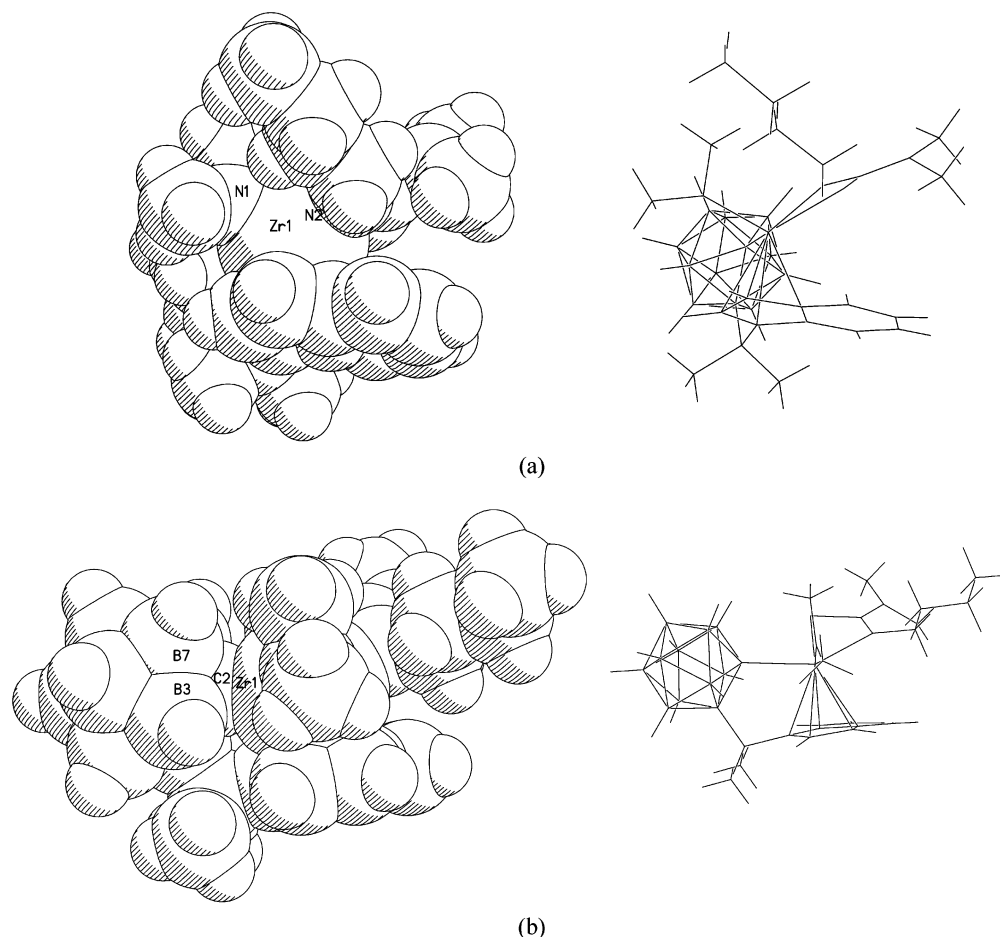


Figure 10. Space-filling drawings of $[\eta^5\text{-}\sigma\text{-Me}_2\text{C}(\text{C}_9\text{H}_6)(\text{C}_2\text{B}_{10}\text{H}_{10})]\text{Zr}(\text{NMe}_2)[\eta^2\text{-SC}(\text{NMe}_2)\text{NBu}^n]$ (**8a**): (a) axial view along the Zr–C(cage) bond; (b) equatorial view.

is dependent upon the availability of the open coordination site of the central Zr atom.

Steric effects are also reflected in the structural variations associated with the bond distances and angles around the Zr center (Table 3). In general, the more crowded coordination environment around the Zr center leads to the longer Zr–C(C₅ ring) and Zr–C(cage) distances and smaller Cent–Zr–C(cage) angles. However, the C(C₅ ring)–A–C(cage) (A = C, Si) angles remain almost unchanged, indicating that the geometry of the linked indenyl–carboranyl ligands is not affected by the inserted groups.

Conclusions

Reactions of $[\eta^5\text{-}\sigma\text{-Me}_2\text{A}(\text{C}_9\text{H}_6)(\text{C}_2\text{B}_{10}\text{H}_{10})]\text{Zr}(\text{NMe}_2)_2$ (A = C (**1a**), Si (**1b**)) with various unsaturated molecules were investigated. Small molecules such as CS₂, PhCN, CH₂=CHCN, ⁿBuNCS, and PhNCO inserted exclusively into the Zr–N bonds to give mono-, di-, and triinsertion products, depending upon the substrates. The Zr–C(cage) bond remains intact in all reactions. It is suggested that the preference of Zr–N over Zr–C(cage) insertion is governed by steric factors.

Compounds **1a,b** initiated the polymerization of CH₂=CHCN to produce poly(acrylonitrile) and catalyzed the trimerization of PhNCO. **1a,b** reacted with methyl methacrylate to afford metal methoxide and CH₂=C(Me)CONMe₂, probably due to the high oxophilicity

of the Zr atom. Possible reaction pathways for these reactions were proposed.

New zirconium compounds were fully characterized by various spectroscopic data, elemental analyses, and single-crystal X-ray diffraction studies. The following common structural features were observed in the insertion products by comparison with their parent compounds **1a,b**: (1) slightly longer Zr–C(C₅ ring) and Zr–C(cage) distances, (2) slightly smaller Cent–Zr–C(cage) angles and similar C(C₅ ring)–A–C(cage) angles (A = C, Si), and (3) some degree of p–π bonding in the X=CNMe₂ (X = N, S) moieties.

Acknowledgment. The work described in this paper was supported by grants from the Research Grants Council of the Hong Kong Special Administration Region (Project No. CUHK 4267/00P) and the National Science Foundation of China through the Outstanding Young Investigator Award Fund (Project No. 20129002).

Supporting Information Available: Tables of crystallographic data and data collection details, atomic coordinates, bond distances and angles, anisotropic thermal parameters, and hydrogen atom coordinates and figures giving atom-numbering schemes for compounds **2a**, **3a**, **4a,b**, **5a,b**, **6a,b**, **7b**, **8a,b**, and **9a**. This material is available free of charge via the Internet at <http://pubs.acs.org>.